International Journal of Undergraduate Research and Creative Activities

Volume 6 Article 2

June 2014

Predicting Creep in Alloy 617 Pressurized Tubes Using Uniaxial Bar Test Data

Joseph Croteau
Department of Materials Science and Engineering, Boise State University, joecroteau@u.boisestate.edu

Allyssa Bateman
Department of Materials Science and Engineering, Boise State University, allyssabateman@u.boisestate.edu

Yudhishthir Bhetwal
Department of Mechanical and Biomedical Engineering, Boise State University, yudhishthirbhetwal@u.boisestate.edu

Theodora Caldwell
Department of Materials Science and Engineering, Boise State University, TheodoraCaldwell@u.boisestate.edu

Justin Allen
Department of Mechanical and Biomedical Engineering, Boise State University, JustinAllen@u.boisestate.edu

See next page for additional authors

Recommended Citation
Croteau, Joseph; Bateman, Allyssa; Bhetwal, Yudhishthir; Caldwell, Theodora; Allen, Justin; and Lindau, Elias (2014) "Predicting Creep in Alloy 617 Pressurized Tubes Using Uniaxial Bar Test Data," *International Journal of Undergraduate Research and Creative Activities*: Vol. 6, Article 2.
DOI: http://dx.doi.org/10.7710/2168-0620.1026

Predicting Creep in Alloy 617 Pressurized Tubes Using Uniaxial Bar Test Data

Peer Review
This work has undergone a double-blind review by a minimum of two faculty members from institutions of higher learning from around the world. The faculty reviewers have expertise in disciplines closely related to those represented by this work. If possible, the work was also reviewed by undergraduates in collaboration with the faculty reviewers.

Abstract
Alloy 617, a nickel-based alloy, is a leading candidate for application in next-generation nuclear plants (NGNPs). Creep, a thermally activated, time-dependent deformation process impacts the lifetime and failure of heat exchangers used at the very high operating temperatures and pressures of such plants. Current methods of testing creep are generally limited to bar specimens in uniaxial tension. In an attempt to correlate uniaxial to multiaxial creep behavior a method to test creep in a pressurized tube was developed. Test specimens were pressurized with argon up to 3.5 MPa, and heated to 950°C. Creep rates were measured as strain rates by tracking diametric changes with time. Parallel experimental and modeling efforts were used to characterize creep behavior in the pressurized tubes. The aim of this research was to use the existing body of knowledge concerning creep in Alloy 617 to develop a model to accurately predict creep in tubular components. Towards this end, a constitutive model was developed and computer simulations undertaken which were ultimately verified experimentally.

Keywords
Alloy 617, creep, next generation nuclear plant, pressure vessel, very high temperature reactor

Acknowledgements
This project was completed as a capstone undergraduate research project, being generously funded by the Idaho National Laboratory and sponsored by Dr. Richard Wright and Jill Wright. The authors wish to especially thank their instructors, Chad Watson and Sarah Haight and our faculty advisors, Drs. Rick Ubic and Steve Tennyson; as well as the many more encouraging personnel at Boise State University, especially Dr. John Youngsman, Dr. Mike Hurley and Brian Jaques. The facilities of Dr. Darryl Butt and the Advanced Material Laboratory, as well as the Boise State Center for Materials Characterization have been greatly appreciated. The authors also wish to express their gratitude to Dr. Brent Davis of Micron Technologies for a gracious donation of test equipment.

Editor's Note: Dr. Rick Ubic, Associate Professor, Department of Materials Science & Engineering, Boise State University, served as faculty mentor for this work.

Authors
Joseph Croteau, Allyssa Bateman, Yudhishthir Bhetwal, Theodora Caldwell, Justin Allen, and Elias Lindau

INTRODUCTION

The next generation nuclear plants included in the Department of Energy's Generation IV Nuclear Energy Systems Programs promise to exceed the performance of current reactor designs. These designs, including the Very High Temperature Reactor (VHTR), have the capability of producing electricity and hydrogen, and recycling discharged fuel. To efficiently do so, the VHTR will require operating temperatures much higher than those of current plants. Secondary heat exchangers in these designs will be exposed to temperatures up to 1000°C and pressures up to 8 MPa (Corwin, 2004). Under these conditions, creep is a major factor in lifetime performance and limits material selections. Alloy 617, a solid-solution strengthened nickel alloy which exhibits excellent thermal stability when compared to other materials of similar strength (Chommette *et al*, 2010), is being investigated as a leading candidate for use in high-temperature designs (Corwin, 2004).

There have been many uniaxial creep studies of Alloy 617 applicable to the design of VHTRs and the results have recently been summarized (Swindeman, Swindeman & Wiju, 2005; Wright, 2006). Many of the mechanisms that strengthen Alloy 617 are lost at the VHTR operating temperatures. The strengthening γ' phase returns to solution near 700°C (Mankins, 1974) and finely dispersed intragranular carbides, which act as microstructural pins, coalesce at grain boundaries to form less effective, chromium-rich $M_{23}C_6$ and molybdenum-rich M_6C type particles (Kihara *et al*, 1980). The migration of such particles from grain interiors likely reduces drag forces acting on dislocations, allowing the material to deform (Green, 1998). Thus, at temperatures above 700°C, both diffusional and dislocation creep mechanisms may be activated in Alloy 617. Evidence of this behavior can be generally observed in microstructural changes such as grain growth (atomic diffusion) and void formation (vacancy diffusion) (Green, 1998). At high temperatures, Alloy 617 exhibits a quickly exhausted region of primary creep (~0.1% strain), very little to no amount of secondary creep, and transitions rapidly into tertiary creep (Chommette *et al*, 2010; Swindeman, Swindman & Wiju, 2005). It is important to note that this is not classic creep behavior.

Reactor design is governed by the American Society of Mechanical Engineers' Boiler and Pressure Vessel code (ASME B&PVc) (ASME, 2013), requiring an accurate method of predicting service life. Alloy 617 is proposed for applications in reactor designs as high as 982°C (Swindeman and Swindeman, 2008); however, authors of the draft code for Alloy 617 have identified further concerns in order to build the most thorough understanding of creep behavior, namely, the combined effects of aging, environment, loading and temperature, as well as the reliability of predicting component behavior from laboratory experiments (Corum and Blass, 1991). There has been significant effort to characterize the uniaxial creep behavior of Alloy 617 (Swindeman, Swindeman & Wiju, 2005), biaxial creep behavior has been tested in thin-walled tubes (Manonukul *et al*, 2005), and its applicability to pressure vessels have been theorized (Jelwan, Chowdhury & Pearce, 2011; Manonukul *et al*, 2005; Penkalla, Nickel and Schubert, 1989; Schubert, Penkalla & Ullrich, 1981). However, uncertainty remains as to how these data relate to the creep behavior in a three-dimensionally stressed pressure vessel (Corum and Blass, 1991; Schubert, Penkalla & Ullrich, 1981). The aim of this research is to use the existing body of knowledge concerning Alloy 617 to develop a method of accurately predicting creep in

tubular components. Towards this end, a constitutive model was developed and computer simulations undertaken, which were ultimately verified experimentally.

METHODS AND MATERIALS

This research took a threefold approach to developing a method of predicting creep: (I) developing a constitutive model of creep derived from uniaxial creep testing, (II) simulating creep in a pressure vessel using finite element modeling (FEM), and (III) verifying predictions with experimentation. Creep tests of both uniaxial and pressurized-tubes made use of the same heat of Alloy 617 plate material with the certified chemical composition given in Table 1. As-received material (Figure 1) showed significant inhomogeneity in grain structure and banding of carbides, believed to be an artifact of processing (Wright, 2006).

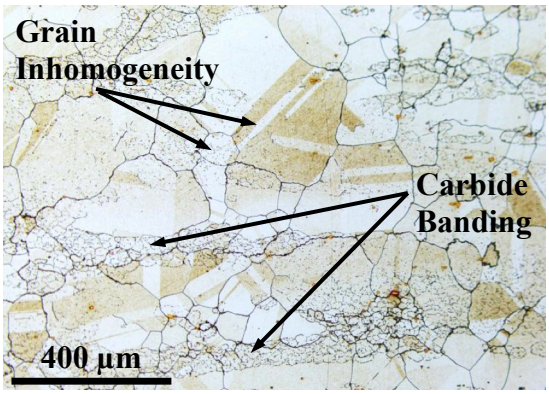

Figure 1. As-received Alloy 617 showing an inhomogeneous grain structure and carbide banding.

Previous work using this heat of Alloy 617 found an average grain size of 150 µm using the linear intercept method (Carrol *et al*, 2013).

The Norton power law for secondary creep was used in this modeling approach to support a later effort to create a minimum-strain-rate dependent time-to-failure model, otherwise known as a Monkman-Grant relationship. The combination of the Norton power law and the Von Mises stress calculation has been previously done with some success (Penkalla, Nickel and Schubert, 1989). The Norton power law is as follows:

$$\dot{\varepsilon}_{min} = A\sigma^n$$

where $A = A_1 exp[-Q_c/RT]$, n is the stress exponent, A_1 is a normalizing factor, and Q_c is the activation energy for creep, all of which are material specific; σ is the applied stress, R is the gas constant and T is the absolute temperature. While appearing quite simple, the normalizing factor and stress exponent in the Norton power law contain information for the many creep mechanisms occurring at a given temperature. The activation energy for creep can be related to the activation energy for diffusion, and has been substituted with the activation energy for self-diffusion in some cases (Swindeman, Swindeman & Wiju, 2005). In general, values of n between 1 and 3 can be taken to suggest diffusional creep, and values between 3 and 5 may suggest dislocation creep as the rate controlling mechanism (Green, 1998). For this reason, the Norton power law can only be applied over a finite range of temperatures where the parameters remain constant for specific creep mechanisms (Courtney, 2000). Since Alloy 617 does not show a significant region of steady-state creep at high temperatures, this investigation is concerned rather with the *minimum* strain rate.

The first step in creating a predictive model was to extract minimum strain rates from twenty existing uniaxial creep tests

Composition of Alloy 617										
Element	Ni	Cr	Co	Mo	Fe	Al	Ti	Mn	Si	C, Cu, S, B
Wt. %	54.1	22.2	11.6	8.6	1.6	1.1	0.4	0.1	0.1	<0.05

Table 1. Certified chemical composition of Alloy 617 from heat QA151053

conducted at the Idaho National Laboratory (INL). These tests ranged in temperature from 800 to 1000°C, and stresses of 16 to 80 MPa. The minimum strain rate was found by fitting the creep curves with a fifth-order polynomial and then minimizing the derivative of this curve was then found to give the minimum strain rate. Plotting the minimum strain rates in a Zener-Hollomon manner as in Figure 2 allows the normalizing factor (A_1) and stress exponent (n) to be extracted in the Norton power law. The results are $A_1 = 2.85\times10^9$ and $n = 5.58$. The activation energy for

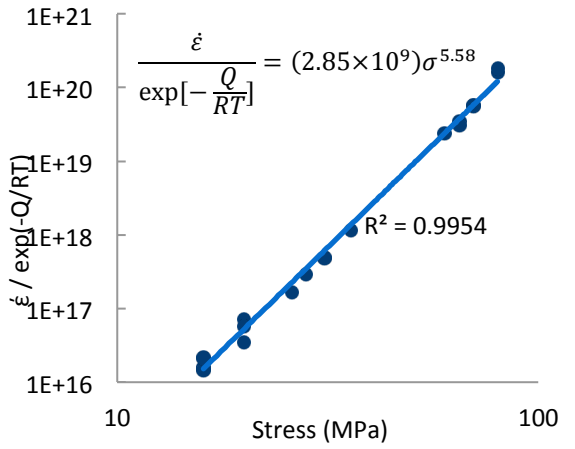

Figure 2. Plotting uniaxial creep data from bar tests allows the parameters used in the Norton power law to be extracted. The normalizing factor, A_1, is given by the coefficient of the fit-line and the stress exponent, n, is given by the slope.

creep, Q_c, was found to be 450 kJ per mole by optimizing the line of best fit. Because data from these tests fall along the same line, the creep mechanism is believed to remain constant for temperatures in the range of 800 to 1000°C; additionally, these parameters should be accurate when predicting creep in a uniaxial bar test. Making the assumption that the stress applied in a uniaxial bar test is analogous to the resulting hoop stress in a pressurized tube, as demonstrated in Figure 3, it is then logical to infer that the linear elongation observed in a bar test is equivalent to the circumferential elongation of a tube, and ultimately, its diametral expansion. Penkalla

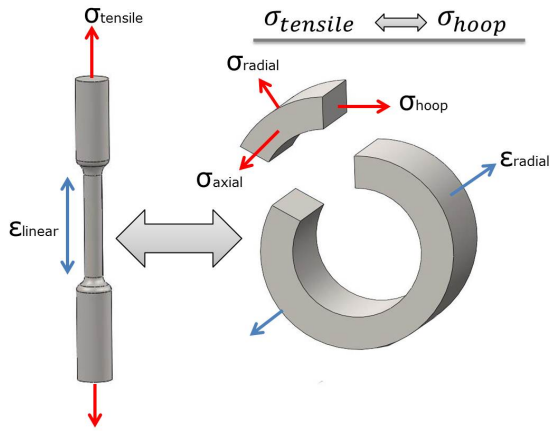

Figure 3. The applied stress in a bar test is assumed to produce the same creep behavior as the resulting hoop stress in a pressurized tube, resulting in diametral creep strain.

et al showed that the application of hoop stress in this way will give a conservative prediction of the strain rate in a thick-walled pressure vessel (Penkalla, Nickel and Schubert, 1989). In other words, equating the linear strain rate to the diametral strain rate should always produce an estimated strain rate that is quicker than what will be observed. This means that a time-to-failure estimate will be shorter than the actual service lifetime.

In addition, finite element modeling (FEM) was used to simulate creep in a manner that is quicker and less expensive than experiments. SolidWorks (Dassault Systèmes SolidWorks Corporation, Waltham, MA), a 3D modeling software, was used to simulate a replica of the tubular test sample. A quarter-model was created with symmetry constraints placed on the cut portions. A default curvature based mesh was applied to the modeled specimen. FEM allowed a static model to verify the Von Mises stress state and the resulting hoop stress in the specimen for given inputs.

Inputting the material specific creep parameters extracted from uniaxial tests and temperature dependent material properties (Special Metals, 2005) allowed a dynamic simulation to be run. The software, also using the Norton power law, produced a time and temperature dependent radial displacement. In addition to modeling creep, FEM was utilized to verify the safety of the designed test specimen, and to ensure that test conditions would result in appreciable levels of creep strain in a reasonable amount of time. Because uniaxial creep tests were not available for 950°C, values for A and n were estimated to be 3.63×10^{-11} and 5.58 respectively; these values lie between the values found for uniaxial creep tests at 900 and 1000°C. Examples of the static and dynamic models are shown in Figure 4. Limitations with the software allowed for a maximum run-time of the dynamic model for 3600 seconds only. The measured strain at this time was used to calculate the strain rate, and was extrapolated to predict creep strains for longer periods of time. The predicted strains from FEM are inherently low, utilizing the minimum strain rate; however, it qualitatively predicts strain in a pressurized tube, meaning it accurately predicts the shape of the crept tube.

To validate the predictions made by the constitutive model and FEM simulation, experimental creep tests were performed on samples of tubular geometry. Because cold-worked Alloy 617 recrystallizes at high temperatures, the code excludes cold-worked material (Corum and Blass, 1991). For this reason, tubular test specimens were machined from solid, solution-annealed, Alloy 617 plate material. This material selection also allows a direct comparison to be made to the bar tests conducted at INL. Specimens were produced in two pieces as shown in Figure 5, and welded together with the dimensions reported in Table 2. The rotational axis of the tubular pieces is in line

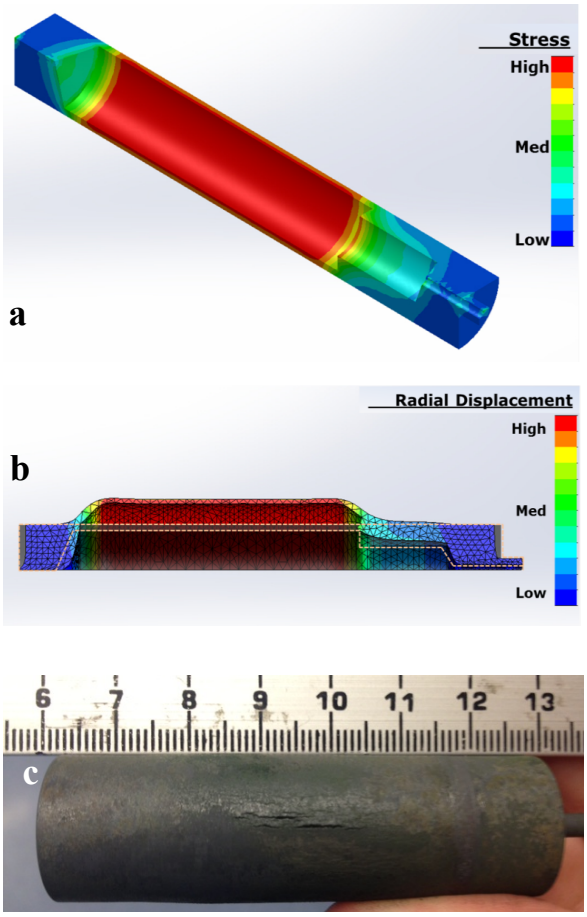

Figure 4. (a) The Von Mises stress state for the pressurized tube specimen, (b) the predicted creep deformation resulting from experimental conditions compared to the original cross-section and (c) a deformed test specimen. Note, FEM values are generalized, but trends are consistent from test to test.

with the rolling direction of the plate. Tests were conducted in a Thermolyne 21100 tube furnace equipped with a Eurotherm 2116 digital controller and a hot zone large enough to incorporate the sample geometry. All tests were conducted at 950°C with internal pressures of either 425 or 500 psi (2.9 and 3.4 MPa). Test parameters are reported in Table 3 along with the results.

The furnace was heated at 5°C per minute, and, after reaching the set dwell time of 37.5 hours, it cooled naturally. The furnace temperature was measured *in-situ* with a K-type thermocouple; although the furnace was set to 950°C, it maintained an

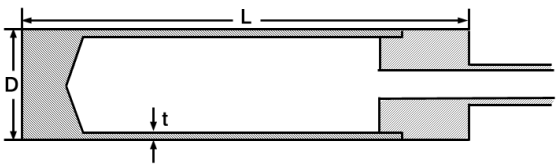

Figure 5. Test samples were machined from solid Alloy 617 in two parts and welded at the butted joint.

Test Sample Geometries			
Designation	Diameter	Length	Thickness
Geometry A	12.70	63.5	0.89
Geometry B	19.05	63.5	1.00

Table 2. Dimensions of experiment samples correspond to Figure 5, with D being diameter, L being length and t being thickness. Given values are in millimeters.

Summary of Results			
Temp (°C)	950	950	950
Geometry	A	B	B
Outer Hoop Stress (MPa)	19.5	23.5	27.7
Predicted $\dot{\varepsilon}_{min}$ (%/hr)	0.0027	0.0079	0.0193
FEM $\dot{\varepsilon}_{min}$ (%/hr)	0.0010	0.0014	0.0024
Experimental $\dot{\varepsilon}_{min}$ (%/hr)	0.0042	0.0014	0.0059

Table 3. Summary of predicted and experimental creep in a pressure vessel.

average of 952°C ± 0.6°C, with boundary temperatures of 951 and 953°C. The inlet tube was welded to a Hastelloy X tube which was attached to stainless steel Swagelok tubing outside of the furnace, allowing the specimens to be internally pressurized using argon (Praxair, 5.0 Ultra High Purity), while the exterior was exposed to laboratory air. This method maintained a constant internal pressure throughout the testing process regardless of the varying specimen geometry resulting from creep deformation. Creep tests were interrupted at regular intervals to measure diametral changes of the samples using a laser scan micrometer (Mitutoyo, LSM-9602), with ± 0.0002 mm precision. Changes in diameter were corrected for oxide growth by subtracting the dimensional changes of the solid region at the end of the sample; any dimensional changes at this location are believed to be a result of high temperature oxidation only, and not from creep. Non-stressed material was placed in the furnace alongside the test specimen to produce material with the same thermal history as the test specimens. Optical and electron microscopy were used to characterize the microstructural changes affecting both thermal- and thermomechanically-aged samples.

RESULTS

The constitutive model built for this alloy assumed the Norton power law and related the applied tensile stress in a uniaxial creep test to the resulting hoop stress in a pressurized tube according to the thick-walled pressure vessel equations. Because this model solves for a minimum creep rate, its predictions are limited to the region of minimum creep only, often called secondary or steady-state creep. The model can be assumed valid for the temperature range of 800 to 1000°C, and can be adapted for geometries included in the thick-walled criteria. Incorporating FEM allows creep studies to be performed rapidly and inexpensively for components of tubular geometries, and offers the advantage of adapting to increasingly complex structures. The predicted minimum strain rates from the constitutive model and FEM, as well as experimentally determined minimum strain rates, for the selected test conditions are summarized in Table 3. The minimum strain rates from the experimental tests were determined in the same way that the uniaxial creep tests were analyzed: by solving for the minimum of the derivative of the creep curve. Experimental results and predicted

creep behavior are plotted together in Figure 6, showing relative agreement between the methods in regards to the magnitude of the creep rates. The minimum

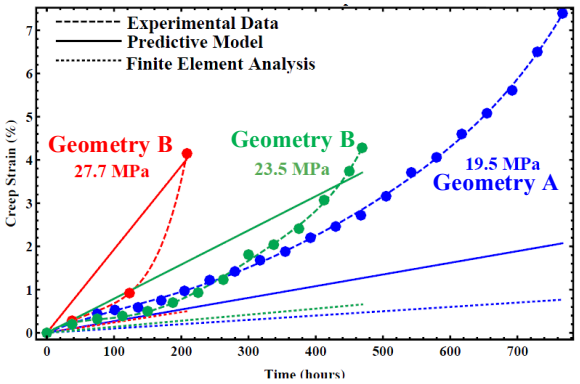

Figure 6. Comparison of experimental with FEA and predictive model results.

strain rates produced by the two models were extrapolated to the full time of the experimental tests to give linear approximations. These approximations are not meant to accurately model the creep curve in its entirety; they should instead predict the linear region of the creep curve. Because the creep of Alloy 617 occurs primarily in the tertiary region at high temperatures, the experimental creep strain quickly diverges from the predicted creep.

Mechanisms that are unique to the radial geometry were observed in addition to the mechanisms of material degradation, which were similar to those previously reported. At elevated temperatures, Alloy 617 forms a passivating chromium oxide, significantly limiting the material lost to corrosion (Corwin, 2004; Wright, 2006). It has been observed previously, as well as in this study, that subsurface aluminum-oxide forms selectively at grain boundaries and can serve as crack-initiators in fatigue tests (Carroll *et al*, 2013). This oxidation is highlighted in Figure 7d, and can be seen to a lesser extent on the interior walls (Figure 7b) which were exposed only to argon at elevated temperatures. It is believed that the diametral expansion of the tested

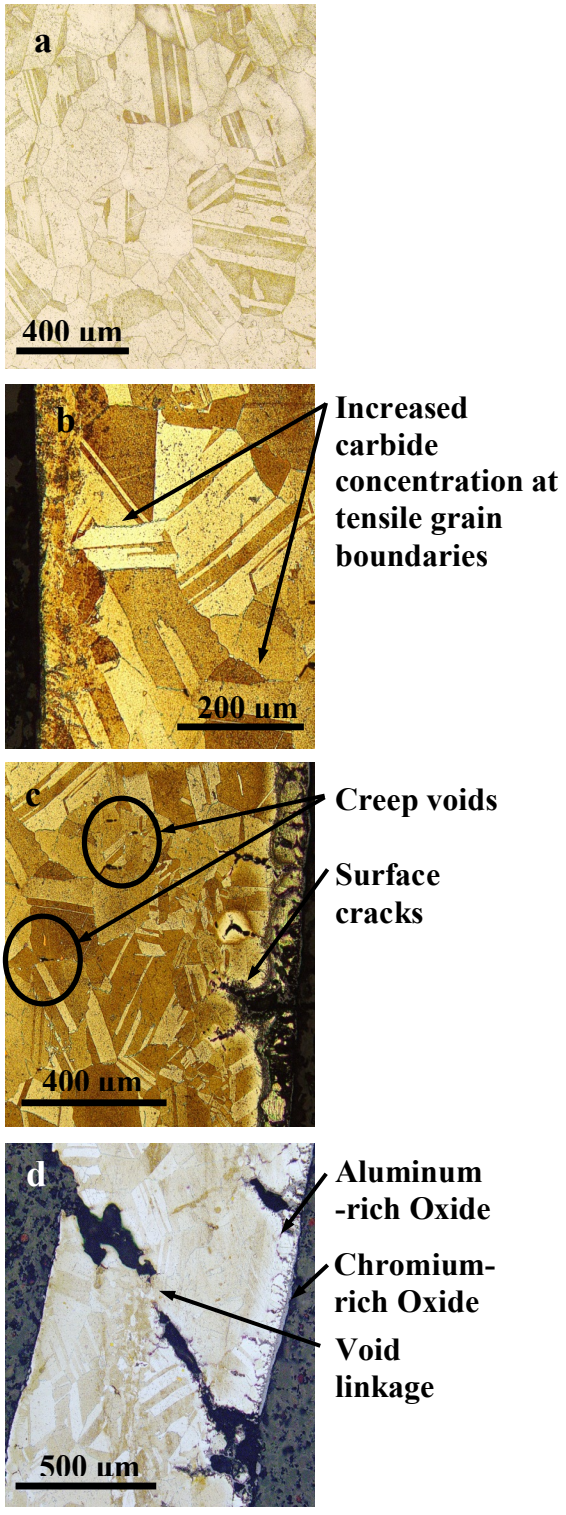

Figure 7. (a) Thermally-aged Alloy 617, (b) increased carbide concentration at tensile grain boundaries, (c) creep void formation and surface cracking in thermomechanically-aged material at ~7% strain and (d) a crack through the wall of a pressurized tube.

tubes opened up cracks in this oxide, leading to the deep oxygen penetration (i.e. not limited to grain boundaries), observed in the crept samples. The cracks which led to the failure of the tube wall propagated at 45° to the wall's normal direction, indicative of a shear failure. It is possible that the reduction of cross-sectional area due to the ingress of surface cracks established a localized area of high shear stress. The linkage of internal creep voids and surface cracks led to the ultimate failure of the tested pressurized tubes (Figure 7d).

DISCUSSION

There are several important distinctions separating the creep tests of bar and tubular geometries which have made the issue at hand a perennial one since the inception of the VHTR designs. A standard uniaxial creep test applies a load in one direction only; whereas a thick-walled pressure vessel is three-dimensionally loaded, with axial, hoop and radial stresses. Relating the combined effects of a multiaxially loaded tube to the observed creep strain is particularly difficult. The failures of the two methods are also marked by uniquely different phenomena. The strain at which a bar test ruptures results in total separation of the two ends. A pressurized tube fails when a single crack is propagated through its wall and the vessel can no longer maintain pressure; using the methods employed by this experiment, this occurrence signaled the end of a test, for no more creep strain could be induced. For this reason, strains at failure of the tested samples were much smaller than a bar test of similar conditions; the strain at failure of the pressurized tubes was about 10 percent of a comparable bar test. This introduces additional restrictions when applying uniaxial data to pressurized tubes; specifically, the strain at failure for a bar test will have little applicability for a pressurized tube. Moreover, data in Figure 4 show that the two tests of the same geometry failed at similar strains despite their different strain rates, and the test of a different geometry failed at a significantly higher strain, suggesting failure may have a dependence on sample geometry in addition to stress and temperature. This raises questions about the applicability of any established time-to-failure models, or of any models which may arise from this study.

Due to the limitations of the experimental setup, *in-situ* dimensional measurements were impractical, and samples had to be cooled and removed from the furnace in order to be measured. It is possible that under these test conditions effects of thermal-fatigue may arise. Realistically, creep-fatigue is a more accurate way to describe the service loads in the reactor components being investigated here, for they will experience cyclic mechanical and thermal loading during start-up and shut-down procedures. Carrol *et al* has shown that two unique methods of failure exist for creep and creep-fatigue of Alloy 617 at 950°C. Fatigue-only tests show transgranular cracking as the primary method of crack propagation (Carroll *et al*, 2013). The introduction of a hold time to produce a creep-fatigue test significantly reduced the cycles to failure, resulting in an intergranular, creep-dominated failure. These tests showed creep void formation on the interior of samples at carbide-rich grain boundaries. Carbide redistribution to grain boundaries increased void formation at carbide-populated grain boundaries, facilitating grain separation, and accelerating void linkage leading to internal cracks several grains in length. Surface cracking initiated at selectively oxidized grain boundaries, in the relatively carbide free region just below the surface, was shown to be a product of fatigue. The detriment to lifetime in creep-fatigue tests can thus be attributed to the synergistic

effect of creep void linkage and surface crack initiation resulting in an accelerated rate of crack propagation (Carroll *et al*, 2013). The fatigue tests in these studies included hundreds of thousands of cycles, whereas the cycles in the present study ranged from three to twenty-one. Although there may be an influence of cyclic loading on the performance of pressurized tubes, their effects are likely not observed in this study where so few cycles were experienced. These issues introduce some doubt when using a purely creep-derived model to predict service life, even if the failure method is creep dominated.

It has been shown that carbides will redistribute by migrating from grain boundaries of high resolved compressive stress, those parallel to the applied load, to the grain boundaries of high resolved tensile and shear stress, those perpendicular and at forty-five degrees to the applied load (Schlegel, 2009). It has been further shown that voids form along the grain boundaries of high resolved tensile and shear stress, frequently accompanied by a high population of carbides (Lillo *et al*, 2009). It is easily imagined that a large fraction of the grain boundaries in a multiaxially loaded system satisfies these criteria for carbide redistribution and void formation. This being true, there are increased numbers of grain boundaries in a pressurized tube likely to exhibit void formation, increasing the number of pathways for voids to link and ultimately accelerating crack propagation in such a system. Observing similar mechanisms in both uniaxial creep tests and in the pressurized tubes further supports, on a physical basis, the use of uniaxial creep data to predict service life in tubular components; however, the aforementioned modes of accelerating creep in pressure vessels must be considered before relating experimental creep measured in bar tests to the creep that is likely to occur in pressurized service components.

Among the simplest of models to describe creep, the Norton power law used here likely oversimplified the test conditions, and did not accurately predict creep in a pressurized tube. Relating the applied stress in a bar test directly to the hoop stress in a pressurized tube was not an entirely valid assumption, for it neglected the effects of axial and radial stresses. This notion is supported by the lack of agreement between the predictive model, which should accurately predict the minimum strain rate in bar tests, and the experimental data. Accounting for the more complex stress state and the mechanisms which possibly accelerate creep in a pressurized tube could help to develop a more sophisticated model for predicting creep. This is not to say that there is no foundation for using uniaxial data to predict creep behavior in a pressure vessel. Using a model derived from uniaxial data, the predicted minimum creep strain rate was within an order of magnitude of what was experimentally measured. Considering the test-to-test variability previously observed in uniaxial creep tests, this is not an unreasonable result.

CONCLUSIONS

Diametral creep was induced and monitored in Alloy 617 pressurized tubes. It was shown that the minimum strain rate from a bar test can be used to predict that in a pressurized tube with some accuracy using the Norton power law and the resulting hoop stress according to the thick-walled pressure vessel equations. In addition to predicting the strain rates, FEM qualitatively predicts the shape of crept tubes. The constitutive model and FEM constructed with parameters specific to Alloy 617 is believed valid for the temperatures 800 to 1000°C where the creep mechanism was shown to remain constant. Further work is needed to

validate the full, and to expand, the temperature range of the present study. To do so, additional tests must be conducted, and creep mechanisms outside this temperature range must be quantified. Characterizing of crept material from tubular samples showed mechanisms previously observed in uniaxial tests, providing some validation for the application of existing uniaxial creep data to service components. This characterization may also prove to be valuable in creating a more sophisticated creep model; accounting for such things as creep void formation, grain growth and the redistribution of carbides. Additional work to refine both the predictive model and FEM may help to construct a more accurate, reliable method of predicting creep in tubular components using data from bar tests. In order to achieve the ultimate goal of a time-to-failure model for pressurized tubes of Alloy-617, a statistical body of data must be furnished.

REFERENCES

American Society of Mechanical Engineers, *Boiler and Pressure Vessel Code 2013 Edition*.

Carroll, L.J., *et al* (2013). The development of microstructural damage during high temperature-creep fatigue of a nickel alloy. *International Journal of Fatigue*, vol. 47, pp. 115-125. DOI: http://dx.doi.org/10.1016/j.ijfatigue.2012.07.016.

Chommette, *et al* (2010). Creep behavior of as received, aged and cold worked Inconel 617 at 850°C and 950°C. *Journal of Nuclear Materials*, vol. 399, pp.266-274. DOI: http://dx.doi.org/10.1016/j.jnucmat.2010.01.019.

Corum, J.M. and Blass, J.J. (1991). Rules for design of Alloy 617 nuclear components to very high temperatures. ORNL, Oak Ridge, Tennessee, USA.

Corwin, W.R. (2004). Updated generation IV reactors integrated materials technology program plan. ORNL/TM-2003/244/R1.

Courtney, T.H. (2000), *Mechanical Behavior of Materials.* Waveland Press, Long Grove, IL, USA.

Green, D.J. (1998). An introduction to the mechanical properties of ceramics. Cambridge University Press, United Kingdom. DOI: http://dx.doi.org/10.1017/CBO9780511623103.

Jelwan, J., Chowdhury, M. and Pearce, G. (2011). Creep life design criterion and its applications to pressure vessel codes. *Materials Physics and Mechanics*, vol. 11, pp. 157-182.

Kihara, S., *et al* (1980). Morphological changes of carbides during creep and their effects on the creep properties in Inconel 617 at 1000°C. *Metallurgical Transactions* 11A, pp. 1019-1031. DOI: http://dx.doi.org/10.1007/BF02654716.

Lillo, T., *et al (2009).* Influence of grain boundary character on creep void formation in Alloy 617. *Metallurgical and Materials Transactions A*, vol. 40A, 2803. DOI: http://dx.doi.org/10.1007/s11661-009-0051-7.

Mankins, W.L., Hosier, J.C. and Bassford, T.H. (1974). Microstructural and phase stability of Inconel Alloy 617. *Metallurgical Transactions,* 5, pp. 2579-2590. DOI: http://dx.doi.org/10.1007/BF02643879.

Manonukul, A., *et al* (2005). Multiaxial creep and cyclic plasticity in nickel-base superalloy C263. *International Journal of Plasticity*, vol. 21, pp. 1-20.

DOI: http://dx.doi.org/10.1016/j.ijplas.2003.12.005.

Penkalla, H.J., Nickel, H. and Schubert, F. (1989). Multiaxial creep of tubes from Incoloy 800 H and Inconel 617 under static and cyclic loading conditions. *Nuclear Engineering and Design*, vol. 112, pp. 279-289. DOI: http://dx.doi.org/10.1016/0029-5493(89)90163-5.

Schlegel, S., *et al (2009).* Precipitate redistribution during creep of Alloy 617. *The Minerals, Metallurgical and Materials Transactions A*, vol. 40A, 2812. DOI: http://dx.doi.org/10.1007/s11661-009-0027-7.

Schubert, F., Penkalla, H.J. and Ullrich, G. (1981). Creep-rupture behavior, a criterion for the design of metallic HTR-components with high application temperatures. *Proc. IAEA Meeting*, Vienna, 5-7 May.

Special Metals (2005). *INCONEL alloy 617,* SMC-029.

Swindeman, R.W. and Swindeman, M.J. (2008). A comparison of creep models for nickel base alloys for advanced energy systems. *International Journal of Pressure Vessels and Piping*, vol. 85, pp. 72-79. DOI: http://dx.doi.org/10.1016/j.ijpvp.2007.06.012.

Swindeman, R.W., Swindeman, M.J. and Wiju, R. (2005). A brief review of models representing creep of Alloy 617. *ASME Vessels and Piping Division Conference*, Denver, CO, USA.

Wright, R.N. (2006). Summary of studies of aging and environmental effects on Inconel 617 and Haynes 230. INL, Idaho Falls, ID, USA. DOI: http://dx.doi.org/10.2172/911722.